

MicroRNA Modification of Coxsackievirus B3 Decreases Its Toxicity, while Retaining Oncolytic Potency against Lung Cancer

Huitao Liu,^{1,7} Yuan Chao Xue,^{1,2} Haoyu Deng,^{1,2,3} Yasir Mohamud,^{1,2} Chen Seng Ng,^{1,2} Axel Chu,⁴ Chinten James Lim,⁴ William W. Lockwood,^{2,5} William W.G. Jia,⁶ and Honglin Luo^{1,2,7}

¹Centre for Heart Lung Innovation, St. Paul's Hospital, Vancouver, BC, Canada; ²Department of Pathology and Laboratory Medicine, University of British Columbia, Vancouver, BC, Canada; ³Department of Vascular Surgery, Renji Hospital, Shanghai Jiaotong University School of Medicine, Shanghai, China; ⁴Department of Pediatrics, University of British Columbia, BC Children's Hospital Research Institute, Vancouver, BC, Canada; ⁵Department of Integrative Oncology, British Columbia Cancer Research Centre, Vancouver, BC, Canada; ⁶Department of Surgery, Division of Neurosurgery, University of British Columbia, Vancouver, BC, Canada; ⁷Department of Experimental Medicine, University of British Columbia, Vancouver, BC, Canada

We recently discovered that coxsackievirus B3 (CVB3) is a potent oncolytic virus against KRAS mutant lung adenocarcinoma. Nevertheless, the evident toxicity restricts the use of wild-type (WT)-CVB3 for cancer therapy. The current study aims to engineer the CVB3 to decrease its toxicity and to extend our previous research to determine its safety and efficacy in treating TP53/RB1 mutant small-cell lung cancer (SCLC). A microRNA-modified CVB3 (miR-CVB3) was generated via inserting multiple copies of tumor-suppressive miR-145/miR-143 target sequences into the viral genome. *In vitro* experiments revealed that miR-CVB3 retained the ability to infect and lyse KRAS mutant lung adenocarcinoma and TP53/RB1-mutant SCLC cells, but with a markedly reduced cytotoxicity toward cardiomyocytes. *In vivo* study using a TP53/RB1-mutant SCLC xenograft model demonstrated that a single dose of miR-CVB3 via systemic administration resulted in a significant tumor regression. Most strikingly, mice treated with miR-CVB3 exhibited greatly attenuated cardiotoxicities and decreased viral titers compared to WT-CVB3-treated mice. Collectively, we generated a recombinant CVB3 that is powerful in destroying both KRAS mutant lung adenocarcinoma and TP53/RB1-mutant SCLC, with a negligible toxicity toward normal tissues. Future investigation is needed to address the issue of genome instability of miR-CVB3, which was observed in ~40% of mice after a prolonged treatment.

INTRODUCTION

Lung cancer is the leading cause of cancer-related death among both men and women worldwide.¹ There are two major forms of lung cancer, non-small-cell lung cancer (NSCLC) and small-cell lung cancer (SCLC), with the former constituting ~85% of all lung cancer cases. Among them, adenocarcinoma is the most common type of lung cancer, responsible for almost half of all lung cancers, and is associated with both smokers and non-smokers.² Genetic mutations play a critical role in the development of lung adenocarcinoma. The well-identified oncogenic driver mutations in lung adenocarcinoma

include those in epidermal growth factor receptor (*EGFR*), anaplastic lymphoma kinase (*ALK*), and Kirsten rat sarcoma viral oncogene homolog (*KRAS*), which occur in ~15%, ~7%, and ~30% of lung adenocarcinoma, respectively.³ SCLC accounts for ~15% of all lung cancers and is almost exclusive to smokers. Between 60% and 90% of SCLC cases feature mutations in gene encoding tumor protein p53 (*TP53^{mut}*) and/or retinoblastoma protein (*RB1^{mut}*).⁴ Although lung adenocarcinoma associated with *EGFR* mutations (*EGFR^{mut}*) or *ALK* translocations can be clinically treated using tyrosine kinase inhibitors,² lung adenocarcinoma with *KRAS* mutations (*KRAS^{mut}*) and SCLC are currently undruggable and associated with a poor prognosis.^{4,5} Highly effective and innovative treatment modalities for these subsets of advanced lung cancer are therefore urgently needed.

Recent advances in oncolytic virotherapy provide a promising new treatment approach.^{6,7} Oncolytic viruses are a group of viruses that are genetically engineered or naturally occurring to specifically destroy cancer cells while sparing normal tissues. Their unique tumor-destructive mechanism lies in their ability of lytic replication, resulting in the lysis of cancer cells and the release of viral progeny to infect neighboring cells. Moreover, oncolytic viruses can overcome the immunosuppressive effects of tumors and have the ability to initiate anti-tumor immunity.^{6,7} In October 2015, the US Food and Drug Administration (FDA) approved the first genetically modified herpes simplex virus 1 (talimogene laherparepvec [T-VEC]) for the treatment of melanoma.⁸ During the past decades, several oncolytic viruses (both RNA and DNA viruses), including coxsackievirus A21,⁹ reovirus,¹⁰ vaccinia virus,¹¹ adenovirus,¹² measles virus,¹³ Newcastle disease virus,¹⁴ and vesicular stomatitis virus,¹⁵ have been

Received 15 August 2019; accepted 7 January 2020;
<https://doi.org/10.1016/j.omto.2020.01.002>

Correspondence: Honglin Luo, Centre for Heart Lung Innovation, St. Paul's Hospital, 1081 Burrard Street, Vancouver, BC V6Z 1Y6, Canada.
E-mail: honglin.luo@hli.ubc.ca



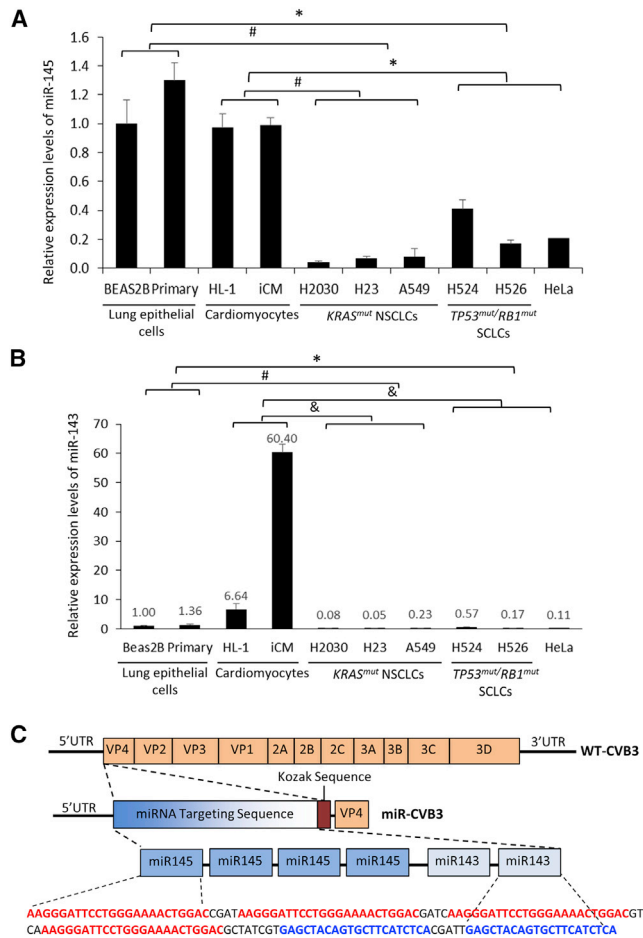


Figure 1. miR-145 and miR-143 Are Significantly Downregulated In Lung Cancer Cells Compared with Normal Lung Epithelial Cells and Cardiomyocytes

(A and B) Expression levels of miR-145 (A) and miR-143 (B) in human normal lung epithelial cells (BEAS2B and primary lung epithelial cells), cardiomyocytes (HL-1 mouse cardiomyocytes and human induced pluripotent stem cell-derived cardiomyocytes [iCMs]), *KRAS*^{mut} non-small-cell lung cancer (NSCLC) cells (H2030, H23, and A549), *TP53*^{mut}/*RB1*^{mut} small-cell lung cancer (SCLC) cells (H524 and H526), and HeLa cells were measured by qRT-PCR and calculated using the equation RQ (relative quantity) = $2^{-\Delta\Delta Ct}$. The results are presented as mean \pm SD (n = 3). One-way ANOVA was used to assess the differences among different cell types. *p < 0.05, #p < 0.01, ^ap < 0.001. (C) Construction of miRNA-modified CVB3 (miR-CVB3). Four copies of miR-145 (5'-AAGGGATTCTGGGAAAACCTGGAC-3') and two copies of miR-143 (5'-GAGCTACAGTGCTTCATCTCA-3') target sequences were inserted between the 5' UTR and VP4 of the CVB3 genome. A Kozak sequence was added before the start codon (ATG) of VP4 to facilitate the translation of viral protein in cancer cells.

tested in clinical trials for the treatment of lung cancer. However, overall anti-cancer efficacy and specificity remain low and there is still no FDA-approved virotherapy for lung cancer.

Coxsackievirus B3 (CVB3) is an enterovirus in the family of Picornaviridae.¹⁶ It is a small, non-enveloped virus that contains a positive

RNA genome encoding a single open reading frame flanked by 5' and 3' untranslated regions (UTRs). Although CVB3 infection can be severe in children and immunocompromised individuals, causing myocarditis, pancreatitis, and meningitis, infection in adults is generally asymptomatic or causes mild flu-like symptoms.¹⁶ Our recent study has demonstrated that CVB3 is an extremely potent oncolytic virus against *KRAS*^{mut} lung adenocarcinoma, while sparing normal lung epithelial cells, and *EGFR*^{mut} lung adenocarcinoma.¹⁷ Despite this promising discovery, we found that wild-type (WT)-CVB3 causes damage to multiple organs, particularly to the heart, in immunodeficient mice.¹⁷

In the current study, we aimed to use microRNA (miRNA) targeting to modify the CVB3 genome to lessen its toxicity to normal tissues while maintaining oncolytic properties specifically in cancer cells. miRNAs are a class of endogenous small non-coding RNAs that are evolutionarily conserved and act as key regulators in a wide range of fundamental cellular functions, including cell proliferation, differentiation, and apoptosis, by binding to the mRNAs with complementary sequences. Subsequently, they promote either mRNA degradation or suppression of translation.¹⁸ Recent evidence suggests that miRNAs also play a key role in tumorigenesis and progression of cancers.^{19,20} miRNAs are commonly downregulated in different types of cancer tissues in comparison with normal tissues.²¹ This unique feature of cancer cells can be exploited to develop miRNA-sensitive, tumor-specific oncolytic viruses. In this study, we showed that inclusion of tumor-suppressive miRNA complementary target sequences into the CVB3 genome markedly reduces its virulence to normal tissues without compromising its anti-tumor potency. Moreover, we demonstrated that, in addition to *KRAS*^{mut} lung adenocarcinoma, CVB3 also acts as a potent oncolytic virus against *TP53*^{mut}/*RB1*^{mut} SCLC.

RESULTS

miR-145 and miR-143 Are Significantly Downregulated in Lung Cancer Cells Compared with Normal Lung Epithelial Cells and Cardiomyocytes

As alluded to above, our recent *in vitro* and *in vivo* studies discovered that WT-CVB3 effectively destroys *KRAS*^{mut} lung adenocarcinoma.¹⁷ Nonetheless, it was observed that the efficient tumor suppression is accompanied by damage to normal tissues, particularly the heart in immunocompromised mice. In this study, we aimed to genetically engineer the CVB3 genome to decrease its toxicity to normal tissues.

The miRNAs miR-145 and miR-143 have been reported to be tumor suppressive and significantly downregulated in lung cancer tissues.^{22,23} To confirm their relative abundance in lung cancer versus normal tissues, quantitative PCR (qPCR) was conducted to measure the levels of miR-145 and miR-143 in various lung cancer and normal cells. As shown in Figures 1A and 1B, the expression of both miR-145 and miR-143 was significantly downregulated in lung cancer cells, including *KRAS*^{mut} lung adenocarcinoma cells (H2030, H23, and A549) and *TP53*^{mut}/*RB1*^{mut} SCLC cells (H524,

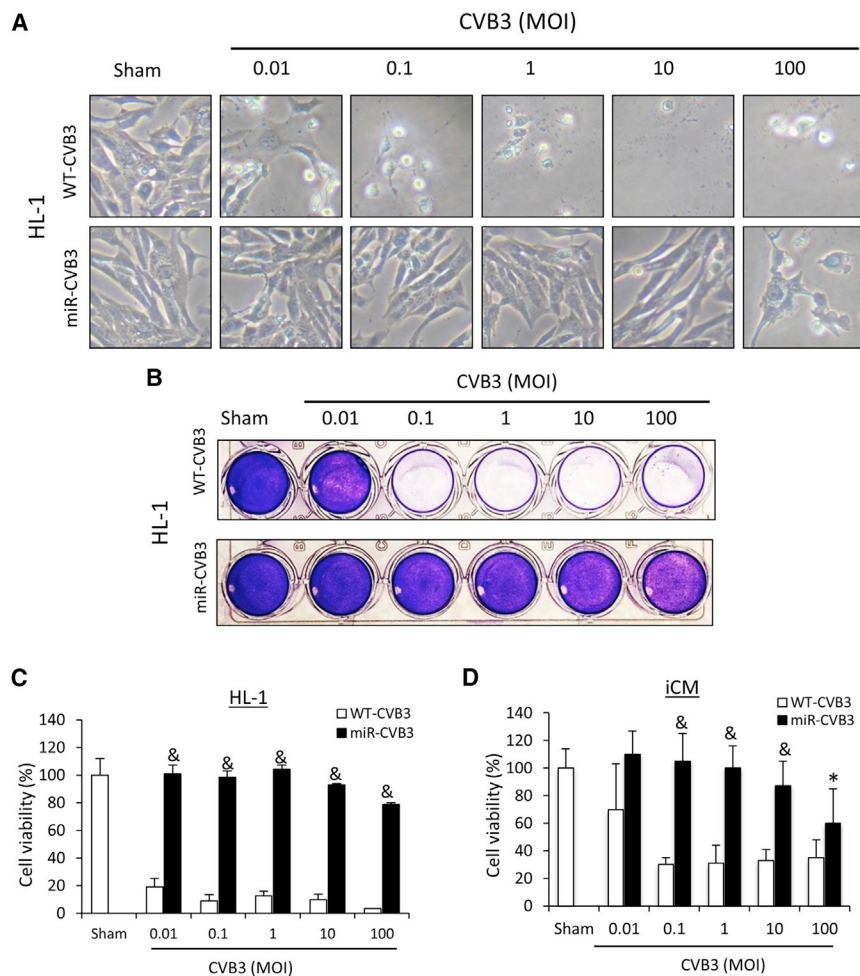


Figure 2. miR-CVB3 Shows a Significantly Reduced Cytotoxicity toward Cardiomyocytes as Compared to WT-CVB3

(A–D) Mouse HL-1 cardiomyocytes (A–C) and human iCMs (D) were sham infected or inoculated with WT-CVB3 or miR-CVB3 at different MOIs as indicated for 72 h. (A) Cell morphology was examined by light microscopy (original magnification, $\times 10$). (B) Cytotoxicity was evaluated by crystal violet staining. (C and D) Cell viability was measured by the alamarBlue assay (mean \pm SD, $n = 3$). An unpaired Student's *t* test was performed for the comparison between the miR-CVB3 and WT-CVB3 groups. * $p < 0.05$, # $p < 0.01$, & $p < 0.001$ compared to WT-CVB3.

we used miRNA (5' UTR)-modified CVB3 (denoted hereinafter by miR-CVB3) to generate virus stocks for subsequent experiments.

miR-CVB3 Shows a Significantly Reduced Cytotoxicity toward Cardiomyocytes

To test the safety of the newly generated recombinant CVB3, we assessed the cytotoxicity of miR-CVB3 toward mouse HL-1 cardiomyocytes, as this cell line has been extensively used to study CVB3-induced cardiac damage,²⁴ and it highly expresses miR-145 and miR-143 (Figures 1A and 1B). After a 72-h viral infection over a range of multiplicity of infection (MOI) of 0.01 to 100, we demonstrated a significant reduction of cytotoxicity in miR-CVB3-treated cells in comparison with WT-CVB3-treated cells, as assessed through morphological observation (Figure 2A), crystal violet staining (Figure 2B), and a cell viability assay (Figure 2C). The decreased cardiotoxicity of miR-CVB3 was further verified in human cardiomyocytes (iCMs) by the cell viability assay (Figure 2D).

miR-CVB3 Retains Its Lytic Potency against *KRAS*^{mut} Lung Adenocarcinoma Cells

We next sought to determine whether inclusion of miRNA targets to the CVB3 genome affects its lytic ability against lung cancer cells. Consistent with our previous observation that *KRAS*^{mut} lung adenocarcinoma cells are acutely permissive to WT-CVB3,¹⁷ we found that WT-CVB3 efficiently killed *KRAS*^{mut} lung adenocarcinoma cells (H2030, H23, A549) in a dose-dependent manner (Figure 3). Moreover, we found that miR-CVB3 retained its ability and potency to lyse *KRAS*^{mut} cells, although at a slightly reduced level compared to WT-CVB3.

Both WT-CVB3 and miR-CVB3 Effectively Induce SCLC Cell Death

As discussed earlier, SCLC is the most aggressive subtype of lung cancer and is associated with poor prognosis.⁴ Most patients with SCLC are diagnosed late when the cancer is already advanced and there is no

H526), than in normal lung epithelial cells (BEAS2B and primary lung epithelial cells) and cardiomyocytes (mouse HL-1 cardiomyocytes and human induced pluripotent stem cell [iPSC]-derived cardiomyocytes [iCMs]). Also note that the levels of miR-145 and miR-143 in HeLa cells, in which WT-CVB3 and miR-CVB3 were grown and titered, were also very low. Our data suggest that miR-145 and miR-143 serve as candidate targets for restricting oncolytic CVB3 replication to tumor cells.

Construction of miRNA-Modified CVB3

We then engineered several miRNA-modified CVB3s, in which multiple copies of miR-145 target sequences alone (either in its forward or reverse orientation) or in combination with miR-143 target sequences (the core sequences of miR-145/miR-143 between mice and humans are 100% identical) were inserted into the 5' UTR or 3' UTR of the CVB3 genome to promote tumor-targeted viral replication. Among them, we found that miRNA-regulated CVB3s, in which four copies of miR-145 and two copies of miR-143 target sequences were inserted into either the 5' UTR or 3' UTR of the CVB3 genome (Figure 1C), displayed the least cardiotoxicity and the highest anti-tumor potency *in vitro* (Figure S1). In this study,

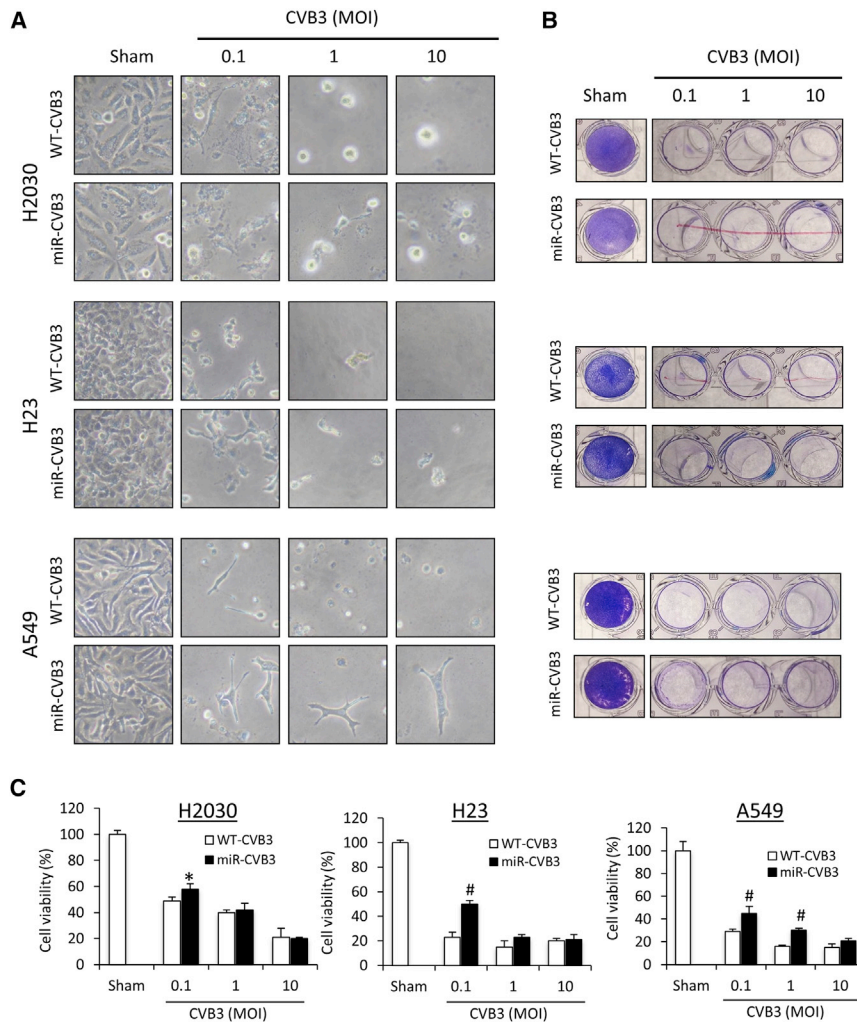


Figure 3. miR-CVB3 Retains the Oncolytic Ability to Infect and Lyse *KRAS*^{mut} Lung Adenocarcinoma Cells Various *KRAS*^{mut} lung cancer cell lines (H2030, H23, and A549) were sham infected or treated with WT-CVB3 or miR-CVB3 at different MOIs as indicated for 72 h. (A) Cell morphology was examined by light microscopy (original magnification, $\times 10$). (B) Cytotoxicity was assessed by crystal violet staining. (C) Cell viability was measured by the alamarBlue assay (mean \pm SD, $n = 3$). An unpaired Student's *t* test was used to compare two groups. * $p < 0.05$, # $p < 0.01$ compared to WT-CVB3.

RNA Levels and Titers of miR-CVB3 Are Significantly Reduced in Normal Lung Epithelial Cells and Cardiomyocytes Compared to WT-CVB3

We further determined whether reduced cytotoxicity in cardiomyocytes and normal lung epithelial cells is a consequence of decreased viral infectivity in these cells. A median tissue culture infection dose (TCID₅₀) assay was performed on supernatant collected from various cell types treated with WT-CVB3 or miR-CVB3 at an MOI of 0.1 for 36 h as indicated to measure infectious viral titers. As shown in Figure 5A, viral titers were strikingly decreased in miR-CVB3-treated HL-1 cardiomyocytes in comparison with WT-CVB3-treated cells. Although a significant decrease in miR-CVB3 titers in H526 *TP53*^{mut}/*RB1*^{mut} cells was also observed, the ratio of reduction was much less as compared to that in cardiomyocytes.

We also examined the kinetics of viral RNA replication (Figure 5B) and titers (Figure 5C) in different cell lines incubated with WT-CVB3 or miR-CVB3 at an MOI of 10 for indicated times by qPCR and a TCID₅₀ assay, respectively. We showed that starting at 5–7 h post-infection, viral RNA copy numbers and titers were considerably lower in miR-CVB3-treated as compared to WT-CVB3-treated HL-1 cardiomyocytes (Figures 5B and 5C, left panels). It was also found that viral RNA copies and titers were decreased in H2030 *KRAS*^{mut} and H526 *TP53*^{mut}/*RB1*^{mut} cells upon miR-CVB3 treatment, but at a much lesser extent (Figures 5B and 5C, middle and right panels). Taken together, these data suggest that the miR-modified version of CVB3 has an increased therapeutic window between cancer and normal cells than does the WT counterpart.

Intraperitoneal Injection of miR-CVB3 Leads to a Significant Reduction of Tumor Volume with Markedly Decreased Cardiotoxicity in Mice

After verification of tumor specificity and efficacy of the miR-CVB3 *in vitro*, we next characterized its safety and effectiveness *in vivo* using a non-obese diabetic (NOD)-severe combined immunodeficiency

targeted therapy for SCLC. In the current study, we extended our previous work on NSCLC to investigate the ability of both WT-CVB3 and miR-CVB3 in killing SCLC. H524 and H526, two SCLC cell lines carrying *TP53/RB1* mutations characteristic of this disease, were utilized in this study. Following a 72-h viral infection at an MOI of 0.1, 1, and 10, both WT-CVB3 and miR-CVB3 caused severe cytopathic effects at all viral doses (Figure 4A). Furthermore, cell viability assays revealed that miR-CVB3 dose-dependently destroyed these cells in a comparable manner to WT-CVB3 (Figure 4B).

Lastly, BEAS2B, a normal human lung epithelial cell line that expresses elevated levels of miR-145 and miR-143 (Figures 1A and 1B), was used to examine the possible cytotoxicity of miR-CVB3 toward normal lung cells. In agreement with our earlier report,¹⁷ infection with WT-CVB3 caused a marginal cytopathic effect and cell death at the higher MOIs examined (Figures 4C and 4D). However, as anticipated, we observed that miRNA modification of CVB3 significantly reduced the toxicity induced by WT-CVB3 to normal lung epithelial cells (Figure 4D).

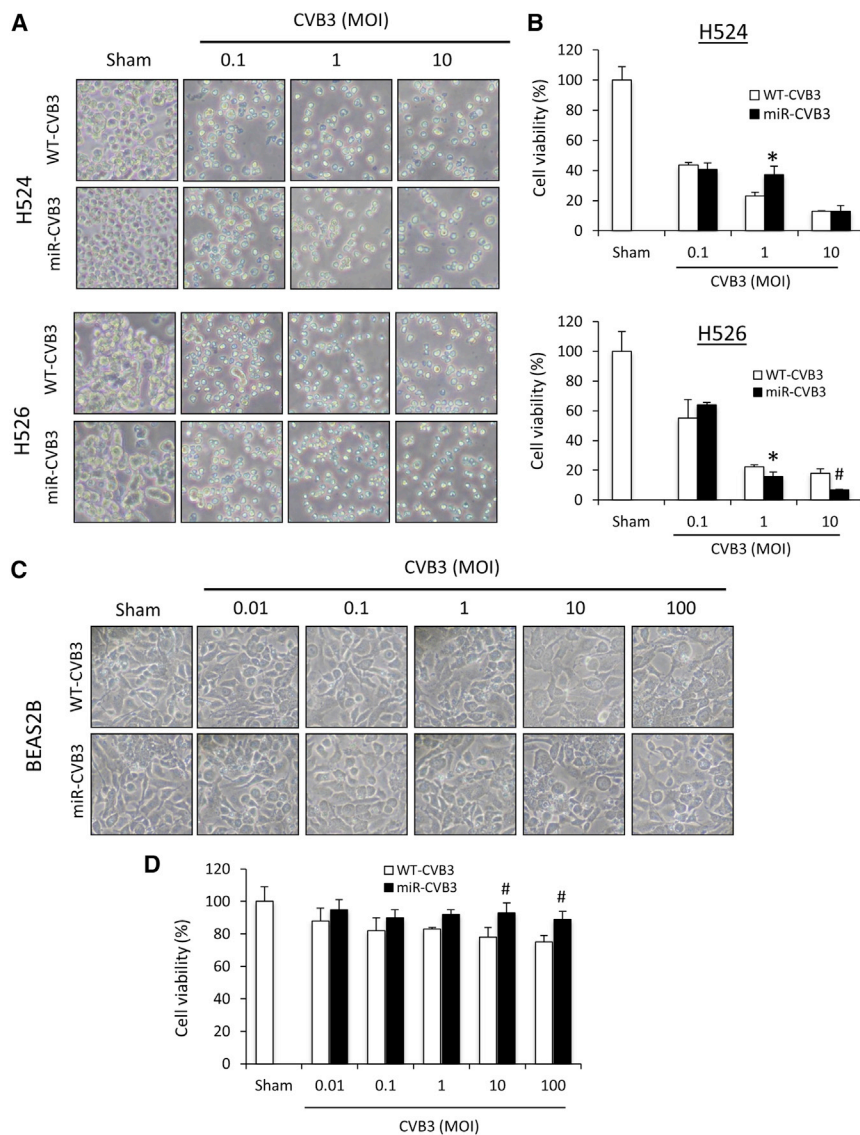


Figure 4. Both WT-CVB3 and miR-CVB3 Potently Destroy SCLC Cells, whereas Human Normal Lung Epithelial Cells Are Not Permissive to Either WT-CVB3 or miR-CVB3

(A–D) *TP53^{mut}/RB1^{mut}* SCLC cell lines (H524 and H526; A and B) and human normal lung epithelial cells (BEAS2B; C and D) were sham infected or inoculated with WT-CVB3 or miR-CVB3 at different MOIs as indicated for 72 h. Cell morphology was examined by light microscopy (original magnification, $\times 10$; A and C). Cell viability was measured by the alamarBlue assay (mean \pm SD, $n = 3$; B and D). An unpaired Student's *t* test was used to assess the difference between cells treated with miR-CVB3 and WT-CVB3. * $p < 0.05$, # $p < 0.01$ compared to WT-CVB3.

(100% survival rate) to the end of the experiment (Figure 6A). Hematoxylin and eosin (H&E) staining (Figure 6B) and pathological quantitation (Figure 6C) revealed a massive inflammatory infiltration and necrosis in the heart of mice treated with WT-CVB3. Remarkably, we observed no apparent cardiac pathology in mice treated with miR-CVB3. There were also no evident damages to other organs, including the lung, liver, and spleen, in both WT-CVB3- and miR-CVB3-treated mice. Modest pancreatic pathology was observed in both groups (Figures 6B and 6C). Viral quantitation by VP1 immunostaining (Figures 6D and 6E) and plaque assay (Figure 6F) demonstrated a significant reduction in viral protein VP1 expression (almost undetectable) and viral titers (i.e., ~ 1 million-fold lower) in the heart of miR-CVB3 mice as compared to WT-CVB3 mice, indicating that decreased cardiovirulence in miR-CVB3 mice is mainly due to reduced viral replication. It was also observed that VP1 expression (nearly undetectable) and viral titers were significantly decreased in the

pancreas of miR-CVB3 mice compared to WT-CVB3 mice (Figures 6D–6F).

(SCID) xenograft mouse model. Since CVB3 infection triggers more severe inflammation in males than in females,²⁵ only male mice were used in this study to determine the oncolytic efficacy and toxicity of miR-CVB3.

We first tested the possible systemic toxicity of miR-CVB3 in NOD-SCID mice without a prior tumor implantation. Mice were intraperitoneally inoculated with either WT-CVB3 ($n = 4$) or miR-CVB3 ($n = 5$) at a single dose of 1×10^8 plaque-forming units (PFU) for 14 days, which represents the peak time of CVB3-induced tissue injuries. Various mouse organs were then harvested for the analysis of tissue damage and viral infection. Consistent with our early report,¹⁷ NOD-SCID mice treated with WT-CVB3 showed severe toxicity, and only one mouse survived (25% survival rate) throughout the time course, while all mice treated with miR-CVB3 survived

pancreas of miR-CVB3 mice compared to WT-CVB3 mice (Figures 6D–6F).

Finally, a different cohort of NOD-SCID mice was used to generate the H526-derived *TP53^{mut}/RB1^{mut}* SCLC xenograft model to determine the anti-tumor potency and the long-term toxicity of miR-CVB3. The mouse model was established through subcutaneous injection of H526 cells (1×10^7 cells) into the left and right flank of the mice. After ~ 10 days, the implanted tumor reached a palpable size. WT-CVB3 or miR-CVB3 was then given via intraperitoneal injection as described above. Mice treated with PBS were used as controls. Similar to the observations made in cultured cells (Figures 1A and 1B), we showed that the levels of miR-145 and miR-143 were significantly lower in implanted SCLC as compared to normal mouse tissues, including heart, pancreas, lung, liver, spleen, kidney, intestine,

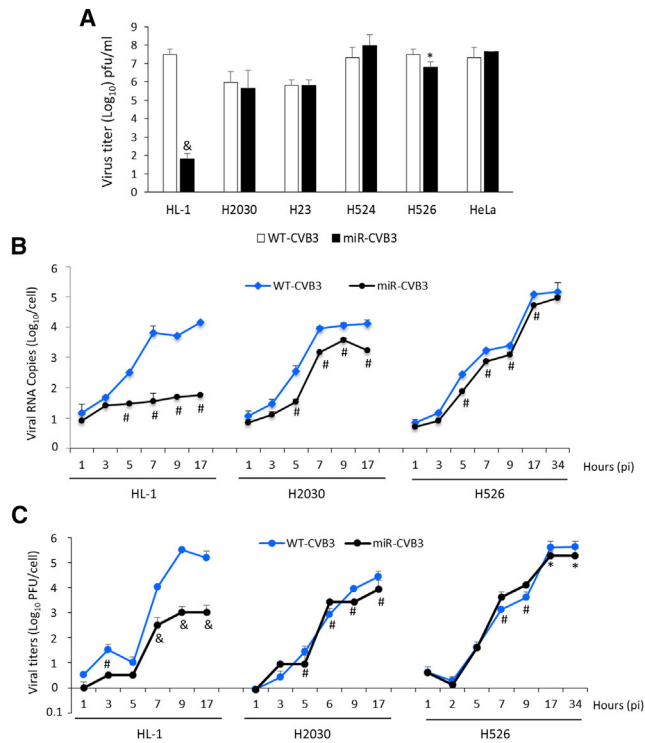


Figure 5. RNA Levels and Titers of miR-CVB3 Are Significantly Reduced in Normal Lung Epithelial Cells and Cardiomyocytes Compared to WT-CVB3 (A–C) Cardiomyocytes (HL-1 mouse cardiomyocytes), *KRAS*^{mut} NSCLC cells (H2030 and H23), *TP53*^{mut}/*RB1*^{mut} SCLC cells (H524 and H526), and HeLa cells were infected with WT-CVB3 or miR-CVB3 at an MOI of 0.1 for 36 h (A) or at an MOI of 10 for various times as indicated (B and C). (A) Supernatants were collected for measurement of viral titers by TCID₅₀, and the results are expressed as mean ± SD (n = 3). (B) Cell lysates after different time points of viral infection were harvested for measurement of viral RNA levels (mean ± SD, n = 3). (C) TCID₅₀ assay was conducted on supernatants collected from infected cells for different time courses to determine viral growth curve (mean ± SD, n = 3). An unpaired Student's t test was conducted to evaluate the difference between miR-CVB3 and WT-CVB3 groups. *p < 0.05, #p < 0.01, &p < 0.001 compared to WT-CVB3.

and brain (Figures 7A and 7B). Kaplan-Meier survival analysis revealed that all mice treated with WT-CVB3 succumbed to death or had to be euthanized due to severe morbidity associated with viral infection at or prior to day 15 post-injection, whereas 100% of miR-CVB3-treated mice survived until day 35 post-infection, and the overall survival rate in the miR-CVB3 group at day 56 post-infection was 57.14% (Figure 7C). In the sham group, six out of eight PBS-treated mice were euthanized prior to day 25 because of the exceeded tumor size (>20 mm in diameter) according to animal care guidelines. Tumor size analysis showed that implanted H526-derived tumors in PBS-treated mice continued to grow until the end of experiment, while upon WT-CVB3 or miR-CVB3 treatment the tumor volumes were markedly reduced in a comparable manner between the two groups (Figure 7D). Tumor weight measurement on day 25 also showed a substantial reduction in mice treated with miR-CVB3 compared with PBS treatment (Figure 7E). Tumor volumes remained

very small or undetectable in miR-CVB3-treated mice until the experimental endpoint (i.e., day 56 post-infection, data not shown). Viral titers were extremely low in the heart and lung, but moderately high in the pancreas and tumor, of mice injected with miR-CVB3 on day 25 (Figure 7F). There was no evident tissue damage in mice treated with miR-CVB3 or PBS on day 25 post-treatment (Figure 7G, pathological scores were not shown due to undetectable pathology). For long-term toxicity analysis (i.e., after day 35 post-infection), we found that mice that survived the entire experimental period (i.e., day 56) displayed no tissue damage and VP1 positive staining, similar to the data shown in Figure 7C. However, evident cardiotoxicity and positive VP1 staining was observed in the heart and pancreas of mice that died between day 35 and 56 post-treatment (Figure S2A). To determine whether the recurrence of cardiotoxicity is due to genome instability of the miR-CVB3, sequencing was conducted, confirming the loss of inserted miRNA target sequences (Figure S2B). Future investigation is needed to address this issue. Taken together, our data suggest that miR-CVB3 retains the oncolytic effectiveness against *TP53*^{mut}/*RB1*^{mut} SCLC, but with substantially decreased tissue toxicity.

DISCUSSION

In this study, we genetically modified the CVB3 genome through a miRNA-targeting approach. Using both *in vitro* cell culture and *in vivo* mouse xenograft models, we demonstrated that miR-CVB3 infection is specific to *KRAS*^{mut} lung adenocarcinoma and *TP53*^{mut}/*RB1*^{mut} SCLC cells with little to no observable damage to normal lung or heart cells, leading to significant tumor regression and improved overall survival. The oncolytic effect of miR-CVB3 is very powerful, as evidenced by the observation that one dose of viral injection through systemic administration results in more than 90% reduction of tumor volume. The advantage of systemic delivery of oncolytic virus is apparent. In addition to being clinically feasible, it also has potential to kill metastatic tumors.

The selection of miR-145/miR-143 for the present study is based on our prior experience using their target sequences to augment tumor selectivity of oncolytic herpes simplex virus-1,^{26,27} and on our current evidence that expression levels of miR-145/miR-143 are particularly low in various types of lung cancer cells in comparison to normal lung epithelial cells and cardiomyocytes. This differential expression pattern enables selective viral replication in lung cancer cells. miR-145/miR-143, together with many other miRNAs, have been revealed to function as tumor suppressors by negatively regulating the expression of multiple oncogenes.²⁸ Oncogenic protein RAS has been shown to transcriptionally suppresses miR-145/miR-143,²⁹ whereas activation of tumor suppressor protein p53 causes upregulation of this miRNA cluster.³⁰

As a RNA virus, the CVB3 genome is less stable than that of DNA viruses. To reduce the potential loss of miRNA target function due to viral RNA mutation, we used different miRNA targets and incorporated multiple copies of individual miRNA target sequences. In addition to the recombinant CVB3 generated by inserting the miRNA

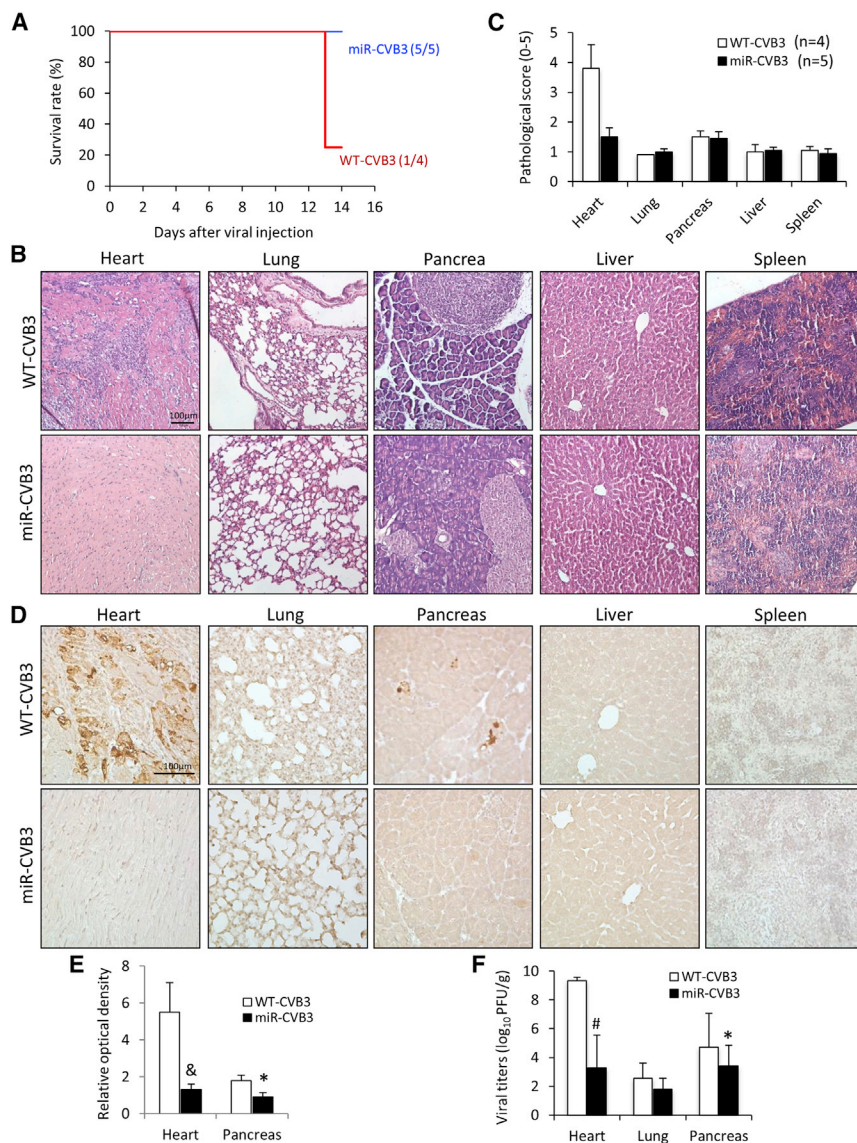


Figure 6. Intraperitoneal Injection of miR-CVB3 Leads to Markedly Decreased Cardiotoxicity in Mice

Male NOD-SCID mice at the age of ~6–8 weeks were inoculated intraperitoneally with one dose of WT-CVB3 (n = 4) or miR-CVB3 (n = 5) at 1×10^8 PFU for 14 days. (A) Kaplan-Meier plot of mouse survival rate. (B–F) Mouse organs were harvested for H&E staining (B), pathological score of the H&E staining in (B) (mean \pm SD) (C), immunohistochemical staining of viral protein VP1 (D), quantitation of VP1 staining (mean \pm SD) (E) in (D) (no positive VP1 staining was detected in the lung, liver, and spleen, and thus only immunostaining in the heart and pancreas was quantified), and plaque assay measurement of viral titers (mean \pm SD) (F). An unpaired Student's t test was performed for the comparison of two groups. * $p < 0.05$, # $p < 0.01$, & $p < 0.001$ compared to WT-CVB3.

by inserting miR-34 target sequences into the 5' UTR and 3' UTR of the viral genome greatly decreases WT virus-induced organ damage and improves mouse survival.³² The differences between our present work and their research include selection of different miRNA target sequences (miR145-miR143 versus miR-34), different route (systemic intraperitoneal versus local intratumoral injection), and frequency (single injection versus multiple injections for up to five times) of viral administration. Despite these differences, both studies provide strong evidence that miRNA-regulated oncolytic CVB3 serves as a valuable tool to be further developed for lung cancer therapy.

We have previously demonstrated that aberrant activation of the ERK1/2 signaling pathway and compromised type I interferon immune response in *KRAS^{mut}* lung adenocarcinoma cells are key factors contributing to the sensitivity to CVB3-induced cell death.³³ This

then opens up the question of what mechanism underlies CVB3 specificity in *TP53^{mut}/RB1^{mut}* SCLC compared to normal cells. *TP53* and *RB1* are the most important and frequently mutated tumor-suppressor genes. Mutations and inactivation of these genes play a key role in the development of various human malignancies. In addition to its best characterized functions in cell cycle arrest and cell death, p53 has also been uncovered to have an antiviral activity through interferon-dependent antiviral immunity and by stimulating apoptosis. It was shown that *TP53* can be transcriptionally activated by type I interferon, a key antiviral mediator, in response to viral infection.³⁴ Studies have further revealed that p53 contributes to innate immune response through promoting interferon-mediated antiviral activity.³⁵ Transgenic mice carrying an extra copy of the *Tp53* gene were found to exhibit increased resistance to viral infection.³⁶ Additionally, p53 has also been reported to

target sequences in their forward orientation (targeting the positive-strand of CVB3) as described in the current study, we also tested the virus modified with reverse-oriented miRNA targets (targeting the negative-strand of CVB3). We found that the cardiotoxicity caused by the former virus at MOIs of 1 and 10 is much less than that of the latter (Figure S1), suggesting that targeting the positive strand of CVB3 is more efficient in reducing viral proliferation and consequent cytotoxicity in normal tissues.

Miyamoto et al.³¹ previously reported that intratumoral injection of WT-CVB3 substantially suppresses NSCLC tumor growth in nude mice without apparent treatment-related toxicity and death. The same research group has since revised their earlier report regarding safety, having shown significant tissue toxicity following WT-CVB3 treatment.³² They further demonstrate that modification of CVB3

then opens up the question of what mechanism underlies CVB3 specificity in *TP53^{mut}/RB1^{mut}* SCLC compared to normal cells. *TP53* and *RB1* are the most important and frequently mutated tumor-suppressor genes. Mutations and inactivation of these genes play a key role in the development of various human malignancies. In addition to its best characterized functions in cell cycle arrest and cell death, p53 has also been uncovered to have an antiviral activity through interferon-dependent antiviral immunity and by stimulating apoptosis. It was shown that *TP53* can be transcriptionally activated by type I interferon, a key antiviral mediator, in response to viral infection.³⁴ Studies have further revealed that p53 contributes to innate immune response through promoting interferon-mediated antiviral activity.³⁵ Transgenic mice carrying an extra copy of the *Tp53* gene were found to exhibit increased resistance to viral infection.³⁶ Additionally, p53 has also been reported to

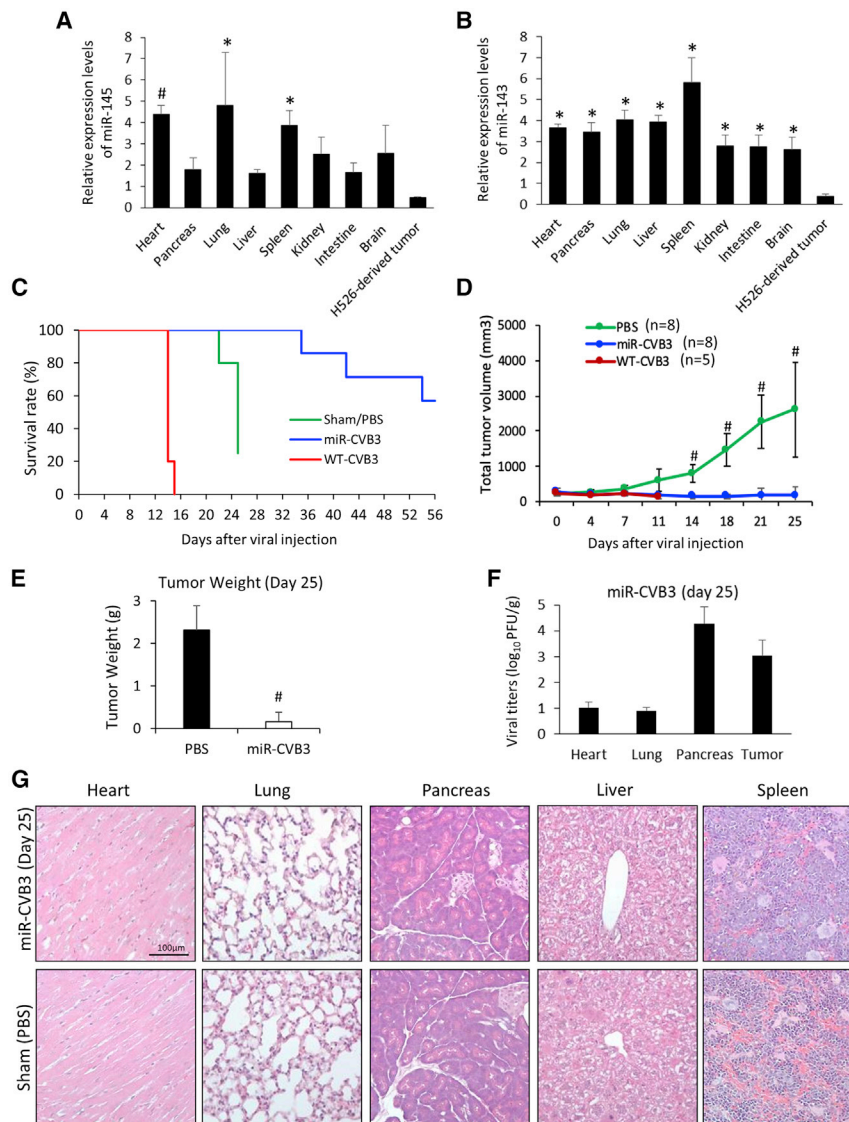


Figure 7. Intra-peritoneal Injection of miR-CVB3

Results in a Significant Reduction of Tumor Volume

A xenograft model was established using H526 SCLC cells in a different cohort of male NOD-SCID mice at ~7 weeks of age as described in [Materials and Methods](#). Once the tumor reached a volume of ~100 mm³, mice were injected intraperitoneally with one dose of PBS (sham, n = 8), WT-CVB3 (1 × 10⁸ PFU, n = 5), or miR-CVB3 (1 × 10⁸ PFU, n = 15; 7 mice were used for long-term survival analysis, and the other 8 mice were euthanized on day 25 post-infection for the measurement of tumor weight, viral titers, and toxicity). (A and B) Expression levels of miR-145 (A) and miR-143 (B) in the heart, pancreas, lung, liver, spleen, kidney, intestine, brain, and H526-derived tumor of PBS-treated mice by qRT-PCR. The results are presented as mean ± SD (n = 3). An unpaired Student's t test was performed for the comparison of the miRNA levels between different mouse tissues and H526 implanted tumors. *p < 0.05, #p < 0.01 compared to implanted tumors. (C and D) Survival rate (Kaplan-Meier plot; C) and tumor volume (mean ± SD; D) were monitored over time as indicated. (E–G) Implanted tumors and various organs were harvested on day 25. Tumor weight (mean ± SD; E) and viral titers (mean ± SD; F) were measured, and H&E staining (G) was conducted. #p < 0.01 as compared to PBS sham controls.

One possible limitation of the miRNA strategy is attenuation of the virulence of modified virus in lung carcinoma cells due to the expression of miRNAs in these cells, although at a considerably lower level as compared to that in normal cells. However, given the wide window of the viral dosages that cause tissue toxicity and kill tumor cells, we expect that a slight increase of viral concentration will overcome this drawback. Another potential issue is the genome instability of the miRNA-modified virus. The loss of the incorporated miRNA target sequences observed in the current study is likely due to the formation of loop structures of the insertion. For cloning purpose, we designed two 14-nt-long sequences containing the PstI and BamHI cut sites, which are reverse complementary to each other, flanking the miR-145/miR-143 modification region in the miR-CVB3. As a consequence, the secondary structure could generate a stem loop covering the region of miRNA modification in both strands of the virus, and subsequently the genetic reversal might happen during genome replication by skipping the region of miRNA modification. Despite the fact that the loss of insertion and consequent recurrence of viral pathogenicity were observed after day 35 of treatment in NOD-SCID mice, it is expected that genetic reversal of miR-CVB3 might be less harmful in immunocompetent mice due to more effective immune clearance of virus as compared to immunocompromised mice. Nonetheless, future research is required to address this problem to minimize the potential risk.

directly inhibit viral transcription. For example, p53 regulates HIV-1 gene expression by suppressing transcriptional activation of the long terminal repeat.³⁷ It was also found that p53 binds to simian virus large T antigen and blocks its function in mediating viral replication.³⁸ Of note, we have previously found that CVB3 infection facilitates p53 degradation, and overexpression of WT-p53 suppresses viral replication.³⁹ Thus, it is conceivable that loss of p53 activity in SCLC cells benefits CVB3 by providing a favorable cellular environment for viral propagation and consequent oncolysis. Similar to *TP53*, the tumor-suppressor gene *RB1* has also been implicated in host immune responses and inflammatory diseases.³⁶ Although the role of *RB1* in viral infection remained to be determined, our early findings that CVB3 infection results in a marked reduction of *RB1* protein expression associated with virus-induced cell growth arrest⁴⁰ point to a viral strategy to counteract the possible antiviral function of *RB1*.

As discussed earlier, both direct oncolysis and anti-tumor immunity triggered by virus infection are thought to contribute to the efficacy of cancer virotherapy.^{6,41,42} The present research focuses mainly on the oncolytic mechanism of miR-CVB3. It is fully recognized there is a lack of data on assessing the role of the host immune system in virotherapy, although NOD-SCID mice lacking functional T and B lymphocytes preserve some natural killer cell and macrophage activity.⁴³ Future research will focus on using immunocompetent transgenic mouse models to evaluate the therapeutic efficacy and safety of the engineered CVB3. We expect that miR-CVB3 will exert an anti-tumor effect by triggering direct tumor lysis and eliciting tumor-specific immunity.

In conclusion, we have generated a recombinant CVB3 with value to be further exploited for the treatment of *KRAS*^{mut} lung adenocarcinoma and *TP53*^{mut}/*RB1*^{mut} SCLC, the two most devastating subtypes of lung cancer.

MATERIALS AND METHODS

Generation of miRNA-Modified CVB3

The miRNA-modified CVB3 (denoted hereinafter by miR-CVB3) was created by insertion of four copies of miR-145 and two copies of miR-143 target sequences into the 5' UTR of the CVB3 genome. The plasmid pCVB3/T7 containing the intact genome of CVB3 (Kandolf strain) was used as the backbone to generate miR-CVB3. Briefly, pCVB3/T7 was digested by XbaI to remove the BamHI sites while sparing the 5' UTR-VP4 region. The resulting plasmid was then mutagenized with a primer (5'-GTT GAT ACT TGA GCT CCC ATT TTG CTG TAT GGA TCC TTT GCT GTA TTC AAC TTA ACA ATG-3') harboring a BamHI site and a Kozak consensus sequence between the 5' UTR and the start codon of VP4. The mutant backbone was further modified by inserting a BamHI-digested PCR product that includes four-copy miR-145 target sequences and a ClaI site amplified using a primer pair (5'-AAT GGA TCC TTA ATT AAC GAA GGG ATT CCT GG-3' and 5'-AAT GGA TCC TTA ATT AAA TCG ATA GCG TCC AGT TTT C-3') from the plasmid pCMV-ICP27-145T.²⁷ The CVB3 genome in the resultant plasmid was then repaired by replacing the BglII-SalI fragment with the corresponding fragment in pCVB3/T7 to construct pCVB3-miR-145. Finally, the plasmid pCVB3-miR-145/miR-143 was generated by a ClaI site insertion of an annealed oligonucleotide pair (5'-cgT GAG CTA CAG TGC TTC ATC TCA CGA TTG AGC TAC AGT GCT TCA TCT CA tta gaa t-3' and 5'-cga ttc tag aTG AGA TGA AGC ACT GTA GCT CAA TCG TGA GAT GAA GCA CTG TAG CTC A-3'), including two copies of miR-143 target sequences. All restriction enzymes used were from Thermo Fisher Scientific.

To produce miR-CVB3 and WT-CVB3 (Kandolf strain) stock, viral genome was synthesized from pCVB3-miR-145/miR-143 and pCVB3/T7 linearized by SalI digestion, respectively, using a HiScribe T7 quick high yield RNA synthesis kit (#E2050S, New England Biolabs). Subsequently, viral RNA was transfected into HeLa cells and the supernatant was collected at ~72 h post-transfection when cytopathic effects were most prominent. The virus-containing super-

natant was further propagated in HeLa cells until viral titers reached desirable levels (i.e., $\sim 5 \times 10^9$ PFU/mL) for storage.

Cell Lines

The *KRAS*^{mut} lung adenocarcinoma cell lines of epithelial origin (i.e., A549 cells [#CCL-185], H2030 cells [#CRL-5914], and H23 cells [#CRL-5800]), the *TP53*^{mut}/*RB1*^{mut} SCLC epithelial cell lines (i.e., H524 cells [#CRL-5831] and H526 cells [#CRL-5811]), and the BEAS2B human normal lung epithelial cell line (#CRL-9609) were all obtained from the American Type Culture Collection. All cells were cultured in Roswell Park Memorial Institute (RPMI) 1640 medium (#11875093, Thermo Fisher Scientific) supplemented with 10% fetal bovine serum (FBS) and 1% penicillin-streptomycin solution. Human primary airway epithelial cells isolated from normal donors were generously provided by Dr. Tillie Hackett at the University of British Columbia.⁴⁴ The HL-1 cardiomyocytes (#SCC065, Sigma-Aldrich) were cultured in Claycomb medium (#51800C, Sigma-Aldrich) as previously described.²⁴ Human cardiomyocytes (iCMs) were generated by differentiation of the human induced pluripotent stem cell line, IPS (IMR90)-1, using the GiWi protocol,⁴⁵ which involved timed inhibition of GSK3 and Wnt signaling. Upon differentiation, the iCMs were maintained in RPMI/B27/insulin media (RPMI 1640 with B-27 supplement complete with insulin [Life Technologies, #17504-044]) through the infection studies.

Animal Studies

The immunocompromised NOD-SCID mice (NOD.CB17-*Prkdc*^{scid}/J, #001303, The Jackson Laboratory) were bred at the Animal Resource Centre of BC Cancer Research Centre. All mouse experiments were conducted at the Centre for Heart Lung Innovation Animal Facility of the University of British Columbia in strict accordance with the recommendation in the *Guide for the Care and Use of Laboratory Animals* (Canadian Council on Animal Care, Ottawa, ON, Canada). The protocol was approved by the University Animal Care Committee (A18-0275).

Two different cohorts of male NOD-SCID mice at the age of ~6–8 weeks were used for this research. The first cohort was conducted to determine the potential systemic toxicity of the viruses. NOD-SCID mice were injected intraperitoneally with a single dose of WT-CVB3 (n = 4 mice) or miR-CVB3 (n = 5 mice) at 1×10^8 PFU in a volume of 100 μ L for 14 days (peak time of virus-induced tissue damage). For the second cohort of the study, H526 cells (1×10^7 cells) were injected subcutaneously into the left and right flank of each mouse to generate the *TP53*^{mut}/*RB1*^{mut} SCLC xenograft mouse model. Once the tumor volume reached a palpable size (~100 mm³ on each side), mice were inoculated with WT-CVB3 (n = 5 mice) or miR-CVB3 (n = 15 mice; 7 mice were used for long-term survival analysis, and the other 8 mice were euthanized on day 25 post-infection for the measurement of tumor weight, viral titers, and toxicity) as described above. Mice treated with an equal volume of PBS (n = 8 mice) were used as controls. The animals were then monitored daily and body weight was measured every 2 days. Tumor size was measured twice weekly until the experimental endpoint, and

tumor volume on each side was calculated as length \times width² \times 0.52 and presented as a total volume of both sides. If the tumor exceeded 20 mm in diameter or mice presented severe symptoms linked to viral infection, the mice were euthanized prior to the experimental endpoint as per the approved animal protocol. Mouse organs, including heart, lung, liver, kidney, spleen, and pancreas, were collected for subsequent analysis.

Quantitative Reverse Transcriptase PCR (qRT-PCR)

Total cellular RNA was extracted using the Monarch total RNA mini-prep kit (#T2010, New England Biolabs). To measure the relative levels of viral RNA, qRT-PCR targeting CVB3 2A, mouse and human GAPDH was performed using the Luna universal one-step qRT-PCR kit (#E3005, New England Biolabs) on a ViiA 7 real-time PCR system (Applied Biosystems). The primer pairs used for viral RNA measurement are as follows: CVB3 2A (forward, 5'-GCT TTG CAG ACA TCC GTG ATC-3'; reverse, 5'-CAA GCT GTG TTC CAC ATA GTC CTT CA-3'), mouse GAPDH (forward, 5'-GGC AAA TTC AAC GGC ACA GT-3'; reverse, 5'-AGA TGG TGA TGG GCT TCC C-3'), and human GAPDH (forward, 5'-AAT CCC ATC ACC ATC TTC CA-3'; reverse, 5'-TGG ACT CCA CGA CGT ACT CA-3'). The CVB3 2A gene level was first normalized to GAPDH mRNA, and then to cell numbers.

To determine the relative expression level of miR-145 and miR-143, three stem-loop primers (miR-145, 5'-CTC AAC TGG TGT CGT GGA GTC GGC AAT TCA GTT GAG AGG GAT TC-3'; miR-143, 5'-GTC GTA TCC AGT GCT GGG TCC GAG TGA TTC GCA CTG GAT ACG ACT GAG CTA CA-3'; and miR-93 [which has been identified as a reference gene for qPCR analysis of miRNA levels^{46,47}], 5'-CTC AAC GGT GTC GTG GAG TCG GCA ATT CAG TTG AGC TAC CTG C-3') were used for RT with an iScript cDNA synthesis kit (#1708890, Bio-Rad) according to the manufacturer's instructions. qPCR was then conducted using three primer pairs targeting miR-145 (forward, 5'-CGG CGG GTC CAG TTT TCC CAG G-3'; reverse, 5'-CTG GTG TCG TGG AGT CGG CAA TTC-3'), miR-143 (forward, 5'-CCT GGC CTG AGA TGA AGC AC-3'; reverse, 5'-CAG TGC TGG GTC CGA GTG A-3'), and miR-93 (forward, 5'-CGG CGG CAA AGT GCT GTT CGT G-3'; reverse, 5'-CTG GTG TCG TGG AGT CGG CAA TTC-3'). Samples were run in triplicate and analyzed using the comparative CT ($2^{-\Delta\Delta CT}$) method with control samples and presented as relative quantitation.

Crystal Violet Assay

Crystal violet staining was performed for assessment of cell death. Briefly, after removal of culture medium and washing with PBS, adherent cells were fixed and stained with 0.4% crystal violet solution for 30 min.

Cell Viability Assay

Cell viability was evaluated using the alamarBlue assay according to the manufacturer's protocol (#BUF012A, Bio-Rad). Briefly, the alamarBlue solution was added to the 48-well plate to a final concentra-

tion of 10%. After incubation at 37°C for 4 h, the absorbance was measured at 570 nm and 600 nm on a microplate reader. Percentage survival of CVB3-infected cells is expressed relative to that of sham controls, which is arbitrarily set as 100% survival.

Viral Titer Quantification

A plaque assay was conducted on CVB3-infected tissue homogenates to assess viral titers as previously reported.⁴⁸ The viral titers were calculated and presented as PFU/g.

The TCID₅₀ assay was performed on supernatant collected from CVB3-infected cells for measuring viral titers as described previously⁴⁹.

Histological Examination

Potential tissue toxicity was evaluated by histological analysis following H&E staining. The pathological score was graded based on inflammation, necrosis, calcification, lesion area, and cellular vacuolization as previously described.⁵⁰

Immunohistochemical Staining

Immunohistochemical staining was performed using the primary antibody of monoclonal anti-CVB3 capsid protein VP1 (1:1,200, Cox mAB 31A2, Mediagnost, Germany) as described previously.⁵¹ VP1 staining was quantified by ImageJ (version 1.0) and presented as relative optical density normalized to sham infection as previously reported.⁵²

Statistical Analysis

All results are expressed as mean \pm standard deviation (SD). Statistical analysis was conducted using one-way ANOVA or an unpaired Student's *t* test as indicated in the figure legends. A value of *p* < 0.05 was considered statistically significant. All results presented are representative of at least three independent experiments.

SUPPLEMENTAL INFORMATION

Supplemental Information can be found online at <https://doi.org/10.1016/j.omto.2020.01.002>.

AUTHOR CONTRIBUTIONS

H. Liu, W.W.G.J., W.W.L., and H. Luo designed the studies. H. Liu, Y.C.X., H.D., Y.M., and C.S.N. performed the experiments. A.C. and C.J.L. generated the iCMs. H. Liu and H. Luo wrote and revised the manuscript.

CONFLICTS OF INTEREST

W.W.G.J. is the Chief Scientific Officer at Virogin Biotech Ltd. H. Liu and C.S.N. are partially sponsored by Virogin Biotech Ltd. through the MITACS Accelerate Program. The remaining authors declare no competing interests.

ACKNOWLEDGMENTS

This work was funded by the BC Lung Association (to H. Luo); the Providence Health Care Research Institute (PHCRI) and Vancouver

Coastal Health Research Institute (VCHRI) Innovation and Translational Research Award (to H. Luo); the Canadian Institutes of Health Research (to W.W.L., PJT-148725); the Terry Fox Research Institute (to W.W.L.); and by the BC Cancer Foundation (to W.W.L.). Y.C.X. and Y.M. are the recipients of a four-year PhD fellowship from the University of British Columbia. W.W.L. is supported by a Michael Smith Foundation for Health Research Scholar Award, a Canadian Institutes of Health Research New Investigator Award, and by an International Association for the Study of Lung Cancer Young Investigator Award.

REFERENCES

- Siegel, R.L., Miller, K.D., and Jemal, A. (2018). Cancer statistics, 2018. *CA Cancer J. Clin.* 68, 7–30.
- Reck, M., and Rabe, K.F. (2017). Precision diagnosis and treatment for advanced non-small-cell lung cancer. *N. Engl. J. Med.* 377, 849–861.
- Ding, L., Getz, G., Wheeler, D.A., Mardis, E.R., McLellan, M.D., Cibulskis, K., Sougnez, C., Greulich, H., Muzny, D.M., Morgan, M.B., et al. (2008). Somatic mutations affect key pathways in lung adenocarcinoma. *Nature* 455, 1069–1075.
- Koinis, F., Kotsakis, A., and Georgoulis, V. (2016). Small cell lung cancer (SCLC): no treatment advances in recent years. *Transl. Lung Cancer Res.* 5, 39–50.
- Tomasini, P., Walia, P., Labbe, C., Jao, K., and Leigh, N.B. (2016). Targeting the KRAS pathway in non-small cell lung cancer. *Oncologist* 21, 1450–1460.
- Bell, J., and McFadden, G. (2014). Viruses for tumor therapy. *Cell Host Microbe* 15, 260–265.
- Lawler, S.E., Speranza, M.C., Cho, C.F., and Chioocca, E.A. (2017). Oncolytic viruses in cancer treatment: a review. *JAMA Oncol.* 3, 841–849.
- Poh, A. (2016). First oncolytic viral therapy for melanoma. *Cancer Discov.* 6, 6.
- (2017). Coxsackievirus A21 synergizes with checkpoint inhibitors. *Cancer Discov.* 7, OF9.
- Villalona-Calero, M.A., Lam, E., Otterson, G.A., Zhao, W., Timmons, M., Subramaniam, D., Hade, E.M., Gill, G.M., Coffey, M., Selvaggi, G., et al. (2016). Oncolytic reovirus in combination with chemotherapy in metastatic or recurrent non-small cell lung cancer patients with KRAS-activated tumors. *Cancer* 122, 875–883.
- Quoix, E., Ramlau, R., Westeel, V., Pappai, Z., Madroszyk, A., Riviere, A., Koralewski, P., Breton, J.L., Stoelben, E., Braun, D., et al. (2011). Therapeutic vaccination with TG4010 and first-line chemotherapy in advanced non-small-cell lung cancer: a controlled phase 2B trial. *Lancet Oncol.* 12, 1125–1133.
- Lei, J., Li, Q.H., Yang, J.L., Liu, F., Wang, L., Xu, W.M., and Zhao, W.X. (2015). The antitumor effects of oncolytic adenovirus H101 against lung cancer. *Int. J. Oncol.* 47, 555–562.
- Fujiyuki, T., Yoneda, M., Amagai, Y., Obayashi, K., Ikeda, F., Shoji, K., Murakami, Y., Sato, H., and Kai, C. (2015). A measles virus selectively blind to signaling lymphocytic activation molecule shows anti-tumor activity against lung cancer cells. *Oncotarget* 6, 24895–24903.
- Meng, S., Zhou, Z., Chen, F., Kong, X., Liu, H., Jiang, K., Liu, W., Hu, M., Zhang, X., Ding, C., and Wu, Y. (2012). Newcastle disease virus induces apoptosis in cisplatin-resistant human lung adenocarcinoma A549 cells in vitro and in vivo. *Cancer Lett.* 317, 56–64.
- Patel, M.R., Jacobson, B.A., Ji, Y., Drees, J., Tang, S., Xiong, K., Wang, H., Prigge, J.E., Dash, A.S., Kratzke, A.K., et al. (2015). Vesicular stomatitis virus expressing interferon- β is oncolytic and promotes antitumor immune responses in a syngeneic murine model of non-small cell lung cancer. *Oncotarget* 6, 33165–33177.
- Fung, G., Luo, H., Qiu, Y., Yang, D., and McManus, B. (2016). Myocarditis. *Circ. Res.* 118, 496–514.
- Deng, H., Liu, H., de Silva, T., Xue, Y., Mohamud, Y., Ng, C.S., Qu, J., Zhang, J., Jia, W.W.G., Lockwood, W.W., and Luo, H. (2019). Coxsackievirus type B3 is a potent oncolytic virus against KRAS-mutant lung adenocarcinoma. *Mol. Ther. Oncolytics* 14, 266–278.
- Bartel, D.P. (2004). MicroRNAs: genomics, biogenesis, mechanism, and function. *Cell* 116, 281–297.
- Gregory, R.I., and Shiekhattar, R. (2005). MicroRNA biogenesis and cancer. *Cancer Res.* 65, 3509–3512.
- Ventura, A., and Jacks, T. (2009). MicroRNAs and cancer: short RNAs go a long way. *Cell* 136, 586–591.
- Lu, J., Getz, G., Miska, E.A., Alvarez-Saavedra, E., Lamb, J., Peck, D., Sweet-Cordero, A., Ebert, B.L., Mak, R.H., Ferrando, A.A., et al. (2005). MicroRNA expression profiles classify human cancers. *Nature* 435, 834–838.
- Guan, P., Yin, Z., Li, X., Wu, W., and Zhou, B. (2012). Meta-analysis of human lung cancer microRNA expression profiling studies comparing cancer tissues with normal tissues. *J. Exp. Clin. Cancer Res.* 31, 54.
- Volinia, S., Calin, G.A., Liu, C.G., Ambs, S., Cimmino, A., Petrocca, F., Visone, R., Iorio, M., Roldo, C., Ferracin, M., et al. (2006). A microRNA expression signature of human solid tumors defines cancer gene targets. *Proc. Natl. Acad. Sci. USA* 103, 2257–2261.
- Wong, J., Zhang, J., Yanagawa, B., Luo, Z., Yang, X., Chang, J., McManus, B., and Luo, H. (2012). Cleavage of serum response factor mediated by enteroviral protease 2A contributes to impaired cardiac function. *Cell Res.* 22, 360–371.
- Fairweather, D., Cooper, L.T., Jr., and Blauwet, L.A. (2013). Sex and gender differences in myocarditis and dilated cardiomyopathy. *Curr. Probl. Cardiol.* 38, 7–46.
- Lee, C.Y., Rennie, P.S., and Jia, W.W. (2009). MicroRNA regulation of oncolytic herpes simplex virus-1 for selective killing of prostate cancer cells. *Clin. Cancer Res.* 15, 5126–5135.
- Li, J.M., Kao, K.C., Li, L.F., Yang, T.M., Wu, C.P., Horng, Y.M., Jia, W.W., and Yang, C.T. (2013). MicroRNA-145 regulates oncolytic herpes simplex virus-1 for selective killing of human non-small cell lung cancer cells. *Virology* 45, 10, 241.
- Shenouda, S.K., and Alahari, S.K. (2009). MicroRNA function in cancer: oncogene or a tumor suppressor? *Cancer Metastasis Rev.* 28, 369–378.
- Kent, O.A., Chivukula, R.R., Mullendore, M., Wentzel, E.A., Feldmann, G., Lee, K.H., Liu, S., Leach, S.D., Maitra, A., and Mendell, J.T. (2010). Repression of the miR-143/145 cluster by oncogenic Ras initiates a tumor-promoting feed-forward pathway. *Genes Dev.* 24, 2754–2759.
- Suzuki, H.I., Yamagata, K., Sugimoto, K., Iwamoto, T., Kato, S., and Miyazono, K. (2009). Modulation of microRNA processing by p53. *Nature* 460, 529–533.
- Miyamoto, S., Inoue, H., Nakamura, T., Yamada, M., Sakamoto, C., Urata, Y., Okazaki, T., Marumoto, T., Takahashi, A., Takayama, K., et al. (2012). Coxsackievirus B3 is an oncolytic virus with immunostimulatory properties that is active against lung adenocarcinoma. *Cancer Res.* 72, 2609–2621.
- Jia, Y., Miyamoto, S., Soda, Y., Takishima, Y., Sagara, M., Liao, J., Hirose, L., Hijikata, Y., Miura, Y., Hara, K., et al. (2019). Extremely low organ toxicity and strong anti-tumor activity of miR-34-regulated oncolytic coxsackievirus B3. *Mol. Ther. Oncolytics* 12, 246–258.
- Deng, H., Fung, G., Qiu, Y., Wang, C., Zhang, J., Jin, Z.G., and Luo, H. (2017). Cleavage of Grb2-associated binding protein 2 by viral proteinase 2A during *Coxsackievirus* infection. *Front. Cell. Infect. Microbiol.* 7, 85.
- Takaoka, A., Hayakawa, S., Yanai, H., Stoiber, D., Negishi, H., Kikuchi, H., Sasaki, S., Imai, K., Shibue, T., Honda, K., and Taniguchi, T. (2003). Integration of interferon- α/β signalling to p53 responses in tumour suppression and antiviral defence. *Nature* 424, 516–523.
- Muñoz-Fontela, C., Macip, S., Martínez-Sobrido, L., Brown, L., Ashour, J., García-Sastre, A., Lee, S.W., and Aaronson, S.A. (2008). Transcriptional role of p53 in interferon-mediated antiviral immunity. *J. Exp. Med.* 205, 1929–1938.
- Muñoz-Fontela, C., Mandinova, A., Aaronson, S.A., and Lee, S.W. (2016). Emerging roles of p53 and other tumour-suppressor genes in immune regulation. *Nat. Rev. Immunol.* 16, 741–750.
- Duan, L., Ozaki, I., Oakes, J.W., Taylor, J.P., Khalili, K., and Pomerantz, R.J. (1994). The tumor suppressor protein p53 strongly alters human immunodeficiency virus type 1 replication. *J. Virol.* 68, 4302–4313.
- Tiemann, F., and Deppert, W. (1994). Stabilization of the tumor suppressor p53 during cellular transformation by simian virus 40: influence of viral and cellular factors and biological consequences. *J. Virol.* 68, 2869–2878.

39. Gao, G., Wong, J., Zhang, J., Mao, I., Shrivah, J., Wu, Y., Xiao, A., Li, X., and Luo, H. (2010). Proteasome activator REG γ enhances coxsackieviral infection by facilitating p53 degradation. *J. Virol.* *84*, 11056–11066.
40. Luo, H., Zhang, J., Dastvan, F., Yanagawa, B., Reidy, M.A., Zhang, H.M., Yang, D., Wilson, J.E., and McManus, B.M. (2003). Ubiquitin-dependent proteolysis of cyclin D1 is associated with coxsackievirus-induced cell growth arrest. *J. Virol.* *77*, 1–9.
41. Ilkow, C.S., Swift, S.L., Bell, J.C., and Diallo, J.S. (2014). From scourge to cure: tumour-selective viral pathogenesis as a new strategy against cancer. *PLoS Pathog.* *10*, e1003836.
42. Miest, T.S., and Cattaneo, R. (2014). New viruses for cancer therapy: meeting clinical needs. *Nat. Rev. Microbiol.* *12*, 23–34.
43. Tournoy, K.G., Depraetere, S., Pauwels, R.A., and Leroux-Roels, G.G. (2000). Mouse strain and conditioning regimen determine survival and function of human leucocytes in immunodeficient mice. *Clin. Exp. Immunol.* *119*, 231–239.
44. Hackett, T.L., Warner, S.M., Stefanowicz, D., Shaheen, F., Pechkovsky, D.V., Murray, L.A., Argentieri, R., Kacic, A., Stick, S.M., Bai, T.R., and Knight, D.A. (2009). Induction of epithelial-mesenchymal transition in primary airway epithelial cells from patients with asthma by transforming growth factor- β 1. *Am. J. Respir. Crit. Care Med.* *180*, 122–133.
45. Lian, X., Zhang, J., Azarin, S.M., Zhu, K., Hazeltine, L.B., Bao, X., Hsiao, C., Kamp, T.J., and Palecek, S.P. (2013). Directed cardiomyocyte differentiation from human pluripotent stem cells by modulating Wnt/ β -catenin signaling under fully defined conditions. *Nat. Protoc.* *8*, 162–175.
46. Niu, Y., Wu, Y., Huang, J., Li, Q., Kang, K., Qu, J., Li, F., and Gou, D. (2016). Identification of reference genes for circulating microRNA analysis in colorectal cancer. *Sci. Rep.* *6*, 35611.
47. Song, J., Bai, Z., Han, W., Zhang, J., Meng, H., Bi, J., Ma, X., Han, S., and Zhang, Z. (2012). Identification of suitable reference genes for qPCR analysis of serum microRNA in gastric cancer patients. *Dig. Dis. Sci.* *57*, 897–904.
48. Deng, H., Fung, G., Shi, J., Xu, S., Wang, C., Yin, M., Hou, J., Zhang, J., Jin, Z.G., and Luo, H. (2015). Enhanced enteroviral infectivity via viral protease-mediated cleavage of Grb2-associated binder 1. *FASEB J.* *29*, 4523–4531.
49. Mohamud, Y., Qu, J., Xue, Y.C., Liu, H., Deng, H., and Luo, H. (2019). CALCO2/NDP52 and SQSTM1/p62 differentially regulate coxsackievirus B3 propagation. *Cell Death Differ.* *26*, 1062–1076.
50. Wang, C., Fung, G., Deng, H., Jagdeo, J., Mohamud, Y., Xue, Y.C., Jan, E., Hirota, J.A., and Luo, H. (2019). NLRP3 deficiency exacerbates enterovirus infection in mice. *FASEB J.* *33*, 942–952.
51. Gao, G., Zhang, J., Si, X., Wong, J., Cheung, C., McManus, B., and Luo, H. (2008). Proteasome inhibition attenuates coxsackievirus-induced myocardial damage in mice. *Am. J. Physiol. Heart Circ. Physiol.* *295*, H401–H408.
52. Xue, Y.C., Ruller, C.M., Fung, G., Mohamud, Y., Deng, H., Liu, H., Zhang, J., Feuer, R., and Luo, H. (2018). Enteroviral infection leads to transactive response DNA-binding protein 43 pathology in vivo. *Am. J. Pathol.* *188*, 2853–2862.